Solvent effect of fluorescence on/off switching of diarylethene linked to excited-state intramolecular proton transfer fluorophore

Solvent effect of fluorescence on/off switching of diarylethene linked to excited-state intramolecular proton transfer fluorophore

Tatsumoto Nakahama, Takayoshi Mukaiyama, Daichi Kitagawa, Seiya Kobatake

Manuscript for publication in *Res. Chem. Intermed.*

Solvent effect of fluorescence on/off switching of diarylethene linked to excited-state intramolecular proton transfer fluorophore

Tatsumoto Nakahama • Takayoshi Mukaiyama • Daichi Kitagawa • Seiya Kobatake*

Department of Applied Chemistry, Graduate School of Engineering, Osaka City University,
3-3-138 Sugimoto, Sumiyoshi-ku, Osaka 558-8585, Japan
E-mail: kobatake@a-chem.eng.osaka-cu.ac.jp, Tel & Fax: +81-6-6605-2797

Abstract Efficient fluorescence on/off switching of a dyad consisting of a photochromic diarylethene and a fluorescence dye based on excited state intramolecular proton transfer (ESIPT) was designed and demonstrated. Diarylethenes linked to (2-(2-methoxy-5-methylphenyl)benzothiazol-6-yl)- and (2-(2-hydroxy-5-methylphenyl)benzothiazol-6-yl)-9,9-dioctylfluorene moieties (**1a** and **2a**, respectively) exhibited fluorescence on/off switching upon alternating irradiation with ultraviolet (UV) and visible light in various solvents. The fluorescence on/off contrast of **2a** was found to be higher than that of **1a** in *n*-hexane because the overlap integral between the absorption spectrum of the diarylethene closed-ring form and the fluorescence spectrum of **2a** is larger than that of **1a**. Diarylethene **2a** exhibited green fluorescence with large Stokes shift in *n*-hexane, which is ascribed to ESIPT process from enol form to keto form. In contrast, the fluorescence of **2a** in *N*,*N*-dimethylsulfoxide (DMSO) was mainly observed as blue fluorescence from enol form, while diarylethene **1a** exhibited blue fluorescence in *n*-hexane and DMSO. The fluorescence on/off contrast of **2a** in *n*-hexane was higher than that in DMSO because of the difference in the spectral overlaps in *n*-hexane and DMSO.

Keywords Photochromism, Fluorescence on/off switching, ESIPT, Diarylethene, Solvent effect

Introduction

Fluorescence-switchable molecules have attracted much attention in various applications, such as sensing materials [1,2], bioimaging materials for super-resolution microscopy [3–5], and single-molecule memory materials [6–11] because their fluorescence intensities and/or colors show sensitive changes in response to various external stimuli. In particular, the fluorescence on/off switching of diarylethenes is widely investigated although various molecules such as green fluorescent protein and carbocyanine dye have been used for the fluorescence switching [12]. Diarylethene is one of the photochromic molecules and exhibits reversible isomerization between two forms upon alternating irradiation with ultraviolet (UV) and visible light [13]. Diarylethenes linked to fluorophores exhibit the fluorescence on/off switching upon alternating irradiation with UV and visible light. Generally, the fluorescence of the fluorophores is observed when the diarylethenes are in their open-ring forms. In contrast, the fluorescence is quenched by an energy transfer from the fluorophore to the diarylethene closed-ring form when the diarylethenes are converted to their closed-ring forms [14,15]. Because the fluorescence on/off switching is based on the resonance energy transfer (RET) from the fluorophore to the diarylethene closed-ring form, high RET efficiency is required for the high fluorescence on/off contrast. RET efficiency depends on various factors: the distance between the donor and the acceptor, donor-acceptor orientation, the fluorescence quantum yield of the donor, and an overlap integral between the absorption spectrum of the acceptor and the fluorescence spectrum of the donor [16]. It is important to select the fluorophore that exhibits the fluorescence spectrum overlapped with the absorption spectrum of the diarylethene closed-ring form.

On the other hand, the fluorophores harnessing the excited state intramolecular proton transfer process (ESIPT) have attracted attention from both theoretical and experimental fields because they show uniquely large Stokes shifted fluorescence (Stokes shifts: 6000–12000 cm^{-1}) without self-reabsorption [17]. In most of the ESIPT fluorescence, the large Stokes shift is attributed to keto form isomerized from enol form at excited state. Park and co-workers reported fluorescence on/off switching with high contrast in a polymer film highly loaded with a diarylethene and an ESIPT fluorophore [18]. The absorption band of the ESIPT fluorophore does not overlap with both absorption bands of the diarylethene open- and closed-ring forms, and the ESIPT fluorescence can overlap with the absorption band of the diarylethene closed-ring form. This has an advantage of using the ESIPT dye for fluorescence switching. Therefore, such system can achieve non-destructive read-out. Moreover, photoswitching and photopatterning of dual-color fluorescence used two different ESIPT fluorophores and one diarylethene was demonstrated [19]. ESIPT fluorophores can largely contribute to fluorescence switching in combination with diarylethenes. In these previous reports, diarylethenes and fluorophores were mixed in polymer films. However, diarylethenes directly linked to the fluorophores are desired because the fluorescence switching properties are greatly affected to ratio of the diarylethene and the fluorophore in the system [15,20]. Although diarylethenes linked to various fluorophores have reported so far [13], there are few reports about diarylethene linked to ESIPT fluorophore

although the efficient fluorescence switching systems consisting of the diarylethenes and the ESIPT fluorophores were reported [21]. Moreover, the fluorescence spectra of ESIPT fluorophores often exhibit solvent effect, which is ascribed to intramolecular hydrogen-bonding between the fluorophores and solvents. It is expected that the fluorescence on/off switching of the diarylethene linked to ESIPT fluorophore exhibits the solvent dependence.

Here, we have synthesized diarylethenes linked to the non-ESIPT and ESIPT fluorophores; 1-(2-methyl-5-(7-(2-(2-methoxy-5-methylphenyl)benzothiazol-6-yl)-9,9-dioctylfluoren-2-yl)thiophen-3-yl)-2-(2-methyl-5-phenylthiophen-3-yl)perfluorocyclopentene (**1a**) and 1-(2-methyl-5-(7-(2-(2-hydroxy-5-methylphenyl)benzothiazol-6-yl)-9,9-dioctylfluoren-2-yl)thiophen-3-yl)-2-(2-methyl-5-phenylthiophen-3-yl)perfluorocyclopentene (**2a**), as shown in **Scheme 1**. 9,9-Dioctyl fluorene moiety, which is a typical fluorophore, was incorporated as a linker because of expectation of large absorption coefficient and high fluorescence quantum yield of the fluorene moiety. Furthermore, solvent effect of the fluorescence on/off switching in long π-conjugation system was investigated.

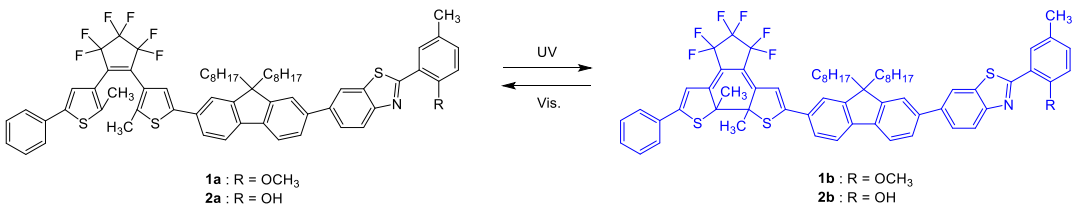

Scheme 1. Diarylethenes used in this work.

Experimental

General

Solvents used were spectroscopic grade and purified by distillation before use. ^{1}H NMR spectra were recorded on a Bruker AV-300N spectrometer at 300 MHz. Deuterated chloroform was used as the solvent and tetramethylsilane (TMS) as an internal standard. Mass spectra were obtained using a JEOL JMS-700T mass spectrometer. High-performance liquid chromatography (HPLC) was conducted using a Hitachi L-7150/L-2400 HPLC system equipped with a Kanto Chemical Mightysil Si60 column. Absorption spectra were measured with a JASCO V-560 absorption spectrophotometer. Fluorescence spectra were measured with a Hitachi F-2700 fluorescence spectrophotometer. All measurements performed in solutions were carried out with optical density around 0.1 at the excitation wavelength in 1 cm path length quartz cells at 298 K. Furthermore, all samples in solutions were deaerated by bubbling with argon gas for 3 min before the measurements.

Photochemical reaction

Photocyclization and cycloreversion quantum yields were determined in *n*-hexane relative to 1,2-bis(2-methyl-5-phenyl-3-thienyl)perfluorocyclopentene [22], whose quantum yield has been previously determined [23]. Photoirradiation was conducted using a 200 W mercury–xenon lamp (Moritex MUV-202) or a 300 W xenon lamp (Asahi Spectra MAX-301) as the light source. Monochromatic light was obtained by passing the light through a monochromator (Jobin Yvon H10 UV). The photocyclization and photocycloreversion reactions were followed by absorption spectra. The samples were not degassed. Photocyclization conversions were determined by absorption spectroscopic analysis.

Fluorescence quantum yield

Fluorescence quantum yields (Φ_f) were determined from the integrated intensity in the fluorescence spectrum of a measurement sample relative to that of a reference solution using eq. 1 [24].

$$\Phi_f = \Phi_{f,ref} \times \frac{A_{ref}}{A} \times \frac{I_{ref}}{I} \times \frac{F}{F_{ref}} \times \frac{n^2}{n_{ref}^2} \quad (1)$$

where A and A_{ref} are the optical densities of the solutions at the excitation wavelength, I and I_{ref} are the excitation light intensities at the excitation wavelength, F and F_{ref} are the integrated intensities of the corrected fluorescence spectra, and n and n_{ref} are the refractive indices of the solvents, used for the sample solution and a standard reference solution, respectively. Anthracene (Φ_f = 0.27 excited at 366 nm in ethanol) [25,26] and 9,10-diphenylanthracene (Φ_f = 0.90 excited at 366 nm in cyclohexane) [27,28] were used as standard references. The Φ_f values were determined as the average of those obtained using two standard references, and the relative experimental error was estimated to be less than 10%.

Materials

Chemicals used for synthesis were commercially available and used without further purification. Compounds **1a** and **2a** were synthesized as shown in **Scheme 2**.

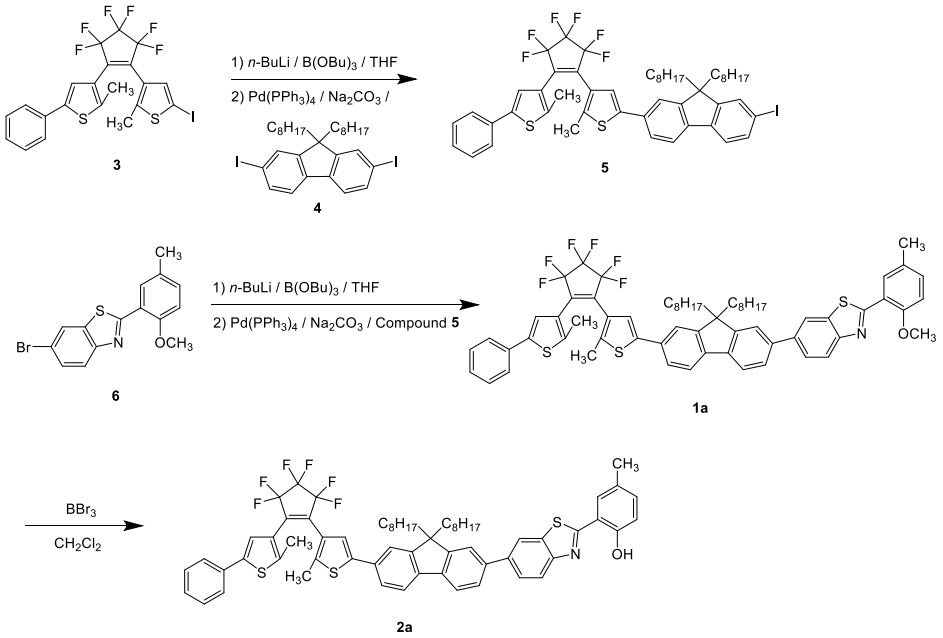

Scheme 2. Synthetic routes of diarylethenes **1a** and **2a**.

*1-(2-Methyl-5-(7-iodo-9,9-dioctylfluoren-2-yl)thiophen-3-yl)-2-(2-methyl-5-phenylthiophen-3-yl)perfluorocyclopentene (**5**)*

Compound **3** (800 mg, 1.4 mmol) [29] was dissolved in anhydrous THF (20 mL) under argon atmosphere. 1.6 M *n*-BuLi hexane solution (1.1 mL, 1.7 mmol) was slowly added dropwise to the solution at −78 °C, and the mixture was stirred for 1.5 h. Tri-*n*-butyl borate (0.45 mL, 1.7 mmol) was slowly added to the solution at −78 °C, and the mixture was stirred for 1.5 h. Adequate amount of distilled water was added to the mixture to quench the reaction. Compound **4** (1.8 g, 2.8 mmol) [30], tetrakis(triphenylphosphine)palladium(0) (49 mg, 0.042 mmol), and 20 wt% Na_2CO_3 aqueous solution (5.0 mL) were added to the solution, and the mixture was refluxed for 33 h. The reaction mixture was neutralized by HCl aqueous solution, extracted with ether, washed with brine, dried over $MgSO_4$, filtered, and concentrated in vacuo. The crude product was purified by column chromatography on silica gel and HPLC using hexane/ethyl acetate (95:5) as the eluent to give 250 mg of **5** in 18% yield. **5**: ^{1}H NMR (300 MHz, $CDCl_3$, TMS) δ = 0.61 (br, 4H, CH_2), 0.81 (t, J = 7 Hz, 6H, CH_3), 1.1–1.2 (m, 20H, CH_2), 1.9–2.0 (m, 4H, CH_2), 2.01 (s, 3H, CH_3), 2.01 (s, 3H, CH_3), 7.3–7.5 (m, 7H, Aromatic H), 7.5–7.6 (m, 3H, Aromatic H), 7.6–7.7 (m, 3H, Aromatic H).

*1-(2-Methyl-5-(7-(2-(2-methoxy-5-methylphenyl)benzothiazol-6-yl)-9,9-dioctylfluoren-2-yl)thiophen-3-yl)-2-(2-methyl-5-phenylthiophen-3-yl)perfluorocyclopentene (**1a**)*

Compound **6** (170 mg, 0.52 mmol) [31] was dissolved in anhydrous THF (10 mL) under argon atmosphere. 1.6 M *n*-BuLi hexane solution (0.39 mL, 0.62 mmol) was slowly added dropwise to the solution at −78 °C, and the mixture was stirred for 1 h. Tri-*n*-butyl borate (0.17 mL, 0.62 mmol) was slowly added to the solution at −78 °C, and the mixture was stirred for 45 min. Adequate amount of distilled water was added to the mixture to quench the reaction. Compound **5** (250 mg, 0.26 mmol), toluene (10 mL), tetrakis(triphenylphosphine)palladium(0) (15 mg, 0.013 mmol), and 20 wt% Na_2CO_3 aqueous solution (4.0 mL) were added to the solution, and the mixture was refluxed for 28 h. The reaction mixture was neutralized by HCl aqueous solution, extracted with ether, washed with brine, dried over $MgSO_4$, filtered, and concentrated in vacuo. The crude product was purified by column chromatography on silica gel and HPLC using hexane/ethyl acetate (70:30) as the eluent to give 60 mg of **1a** in 55% yield. **1a**: ^{1}H NMR (300 MHz, $CDCl_3$, TMS) δ = 0.71 (br, 4H, CH_2), 0.79 (t, J = 7 Hz, 6H, CH_3), 1.1-1.2 (m, 20H, CH_2), 2.0-2.1 (m, 4H, CH_2), 2.02 (s, 3H, CH_3), 2.03 (s, 3H, CH_3), 2.43 (s, 3H, CH_3), 4.06 (s, 3H, OCH_3), 7.00 (d, J = 9 Hz, 1H, Aromatic H), 7.2-7.5 (m, 7H, Aromatic H), 7.5-7.9 (m, 8H, Aromatic H), 8.2-8.3 (m, 2H, Aromatic H), 8.38 (d, J = 2 Hz, 1H, Aromatic H); ^{13}C NMR (75 MHz, $CDCl_3$, TMS) δ = 14.1, 14.6, 14.6, 20.5, 22.6, 23.7, 29.1, 29.2, 29.9, 31.8, 40.3, 55.4, 55.9, 111.8, 119.4, 119.8, 120.2, 120.2, 121.7, 121.9, 122.1, 122.4, 122.7, 124.6, 125.6, 125.7, 125.9, 125.9, 126.4, 127.9, 129.0, 129.5, 130.6, 132.1, 132.5, 133.3, 137.0, 138.3, 139.8, 140.0, 140.7, 141.0, 141.3, 142.2, 142.9, 151.5, 151.7, 152.0, 155.4, 163.6; HR-MS(FAB): m/z = 1086.4211 ($[MH]^+$). Calcd for $C_{65}H_{66}F_6NOS_3$ = 1086.4211.

*1-(2-Methyl-5-(7-(2-(2-hydroxy-5-methylphenyl)benzothiazol-6-yl)-9,9-dioctylfluoren-2-yl)thiophen-3-yl)-2-(2-methyl-5-phenylthiophen-3-yl)perfluorocyclopentene (**2a**)*

Compound **1a** (30 mg, 0.028 mmol) was dissolved in anhydrous dichloromethane (2.0 mL) under argon atmosphere at −78 °C. Boron tribromide (28 mg, 0.11 mmol) was slowly added dropwise to the solution, and the mixture was stirred overnight. Adequate amount of distilled water was added to the mixture to quench the reaction. The reaction mixture was extracted with dichloromethane, washed with brine, dried over $MgSO_4$, filtered, and concentrated in vacuo. The crude product was purified by column chromatography on silica gel and HPLC to give 15 mg of **2a** in 48% yield. **2a**: ^{1}H NMR (300 MHz, $CDCl_3$, TMS) δ = 0.70 (br, 4H, CH_2), 0.79 (t, J = 7 Hz, 6H, CH_3), 1.1–1.2 (m, 20H, CH_2), 2.0–2.1 (m, 4H, CH_2), 2.02 (s, 3H, CH_3), 2.03 (s, 3H, CH_3), 2.38 (s, 3H, CH_3), 7.03 (d, J = 9 Hz, 1H, Aromatic H), 7.2–7.8 (m, 16H, Aromatic H), 8.06 (d, J = 9 Hz, 1H, Aromatic H), 8.16 (d, J = 2 Hz, 1H, Aromatic H), 12.3 (s, 1H, OH); ^{13}C NMR (75 MHz, $CDCl_3$, TMS) δ = 14.1, 14.6, 14.7, 20.5, 22.6, 23.7, 29.1, 29.2, 29.9, 31.8, 40.3, 55.4, 116.4, 117.7, 119.7, 119.8, 120.2, 120.3, 121.7, 122.2, 122.2, 122.4, 124,7, 125.6, 125.9, 125.9, 126.4, 127.9, 128.3, 128.8, 129.0, 132.2, 133.3, 133.5, 133.8, 139.3, 139.4, 140.1, 140.6, 141.1, 141.3, 142.3,

142.9, 151.2, 151.8, 152.0, 155.8, 169.4; HR-MS(FAB): *m*/*z* = 1072.4066 ($[MH]^+$). Calcd for $C_{64}H_{64}F_6NOS_3$ = 1072.4054.

Results and discussion

Photochromism

Fig. 1 shows the absorption and fluorescence spectral changes of **1a** and **2a** in *n*-hexane upon alternating irradiation with UV and visible light (> 500 nm). The optical properties are summarized in **Table 1**. The absorption maximum wavelengths (λ_{abs}) of **1a** and **2a** were observed at 357 and 366 nm (ε = 79400 and 72200 M^{-1} cm^{-1}), respectively. Upon irradiation with 313 nm light, the colorless solution turned blue, and the new absorption band appeared at 593 nm for both **1b** and **2b**. The ε values of **1b** and **2b** isolated by HPLC were determined to be 24400 and 24000 M^{-1} cm^{-1}, respectively. The absorption spectral changes are ascribed to the photoisomerization from the open- to the closed-ring forms. Upon irradiation with visible light, the solution colors and absorption spectra returned to the initial states. Thus, **1a** and **2a** underwent reversible photochromic reactions upon alternating irradiation with UV and visible light. The photocyclization conversions upon irradiation with 313 nm light were determined to be 98 and 96% for **1a** and **2a**, respectively. Moreover, the photocyclization quantum yields ($\Phi_{o\rightarrow c}$) were estimated to be 0.60 and 0.20 for **1a** and **2a**, respectively. The $\Phi_{o\rightarrow c}$ value of **2a** is smaller than that of **1a**. It is attributed to the competition between the photocyclization reaction and the ESIPT process. In contrast, the photocycloreversion quantum yields ($\Phi_{c\rightarrow o}$) were determined to be 0.0047 and 0.0055 for **1a** and **2a**, respectively. This indicates that the excited energy of the diarylethene closed-ring form in **2b** is not transferred to the enol form at the excited state because of the lower energy level of the closed-ring form at the excited state.

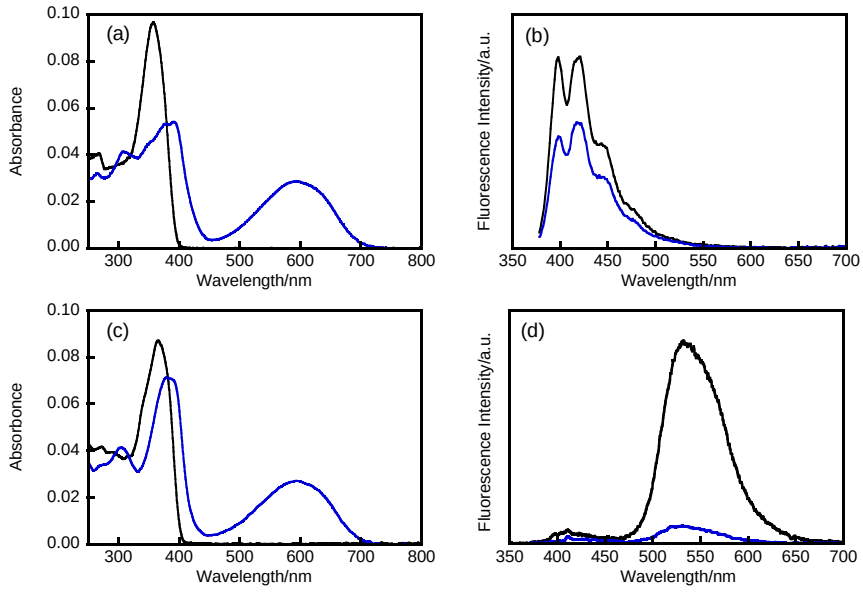

Fig. 1. Absorption and fluorescence spectral changes of **1a** (a, b) and **2a** (c, d) (1.2×10^{-6} mol L^{-1}) in *n*-hexane: the open-ring form (black line), the photostationary solution upon irradiation with 313 nm light (blue line). The fluorescence spectra were recorded upon excitation at 366 nm.

Table 1. Optical properties of diarylethenes in *n*-hexane.

	Open-ring form (**a**)		Closed-ring form (**b**)		$\Phi_{o\rightarrow c}$ [a]	$\Phi_{c\rightarrow o}$ [b]	Conv.[c] /%	λ_{flu} [d] /nm	Φ_f [e]
	λ_{abs}/nm	ε/M^{-1}cm^{-1}	λ_{abs}/nm	ε/M^{-1}cm^{-1}					
1	357	79400	593	24400	0.60	0.0047	98	398	0.015
2	366	72000	593	24000	0.20	0.0055	96	534	0.010

[a]Upon irradiation with 313 nm light. [b]Upon irradiation with 590 nm light. [c]Conversion from the open- to the closed-ring forms upon irradiation with 313 nm light. [d]Excited at 366 nm. [e]Fluorescence quantum yield in *n*-hexane when the diarylethene is in the open-ring form.

Fluorescence properties

As shown in **Fig. 1**, the blue fluorescence of **1a** and green fluorescence of **2a** were observed in *n*-hexane. The fluorescence maximum wavelengths (λ_{flu}) of **1a** and **2a** were 398 and 534 nm, respectively. The Stokes shift of **2a** was 8600 cm^{-1}, which was much larger than that of **1a** (2890 cm^{-1}). This is ascribed to the ESIPT process from enol to keto forms of (2-(2-hydroxy-5-methylphenyl)benzothiazol-6-yl)-9,9-dioctylfluorene moiety, as shown in **Fig. 2a** [31]. The Φ_f values of **1a** and **2a** were determined to be 0.015 and 0.010, respectively. The Φ_f value of **2a** is smaller than that of **1a**. Φ_f of the keto form of the typical ESIPT molecules is low because of the presence of various non-radiative deactivation pathways of keto form at the excited state [17].

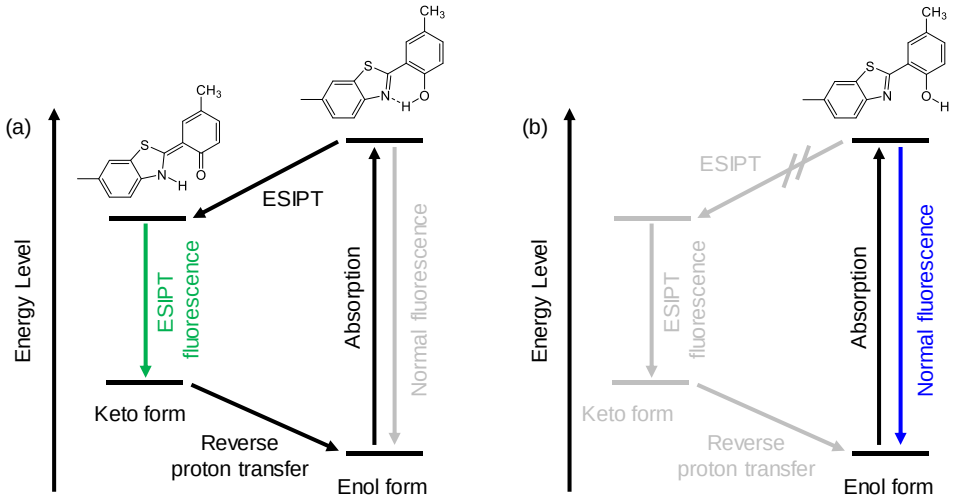

Fig. 2. Schematic illustration of ESIPT process in non-polar solvent (a) and polar solvent (b).

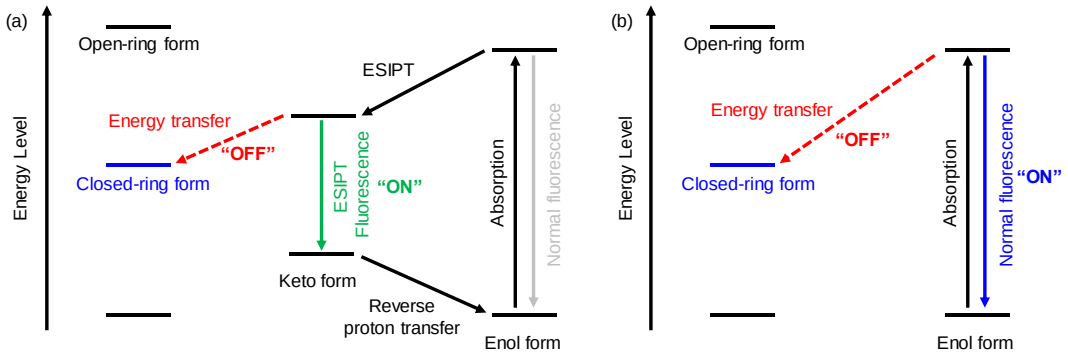

Fig. 3. Schematic illustration of ESIPT and RET process in non-polar solvent (a) and polar solvent (b).

Fluorescence on/off switching

Upon irradiation with 313 nm light, the fluorescence intensity of **1a** and **2a** decreased with increasing photocyclization conversion of diarylethene as shown in **Figs. 1c** and **d**. This is ascribed to the energy transfer from the fluorophore moiety to the diarylethene closed-ring form, as shown in **Fig. 3a** for **2a**. Moreover, the fluorescence intensity returned to the initial one upon irradiation with visible light. These results indicate that **1a** and **2a** showed fluorescence on/off switching upon alternating irradiation with UV and visible light. The fluorescence of **2a** was almost quenched at PSS though **1a** exhibited the residual fluorescence at PSS. The fluorescence on/off contrast is defined as the value of the total area of the initial fluorescence spectrum divided by that of the fluorescence spectrum at PSS. The contrast value of **2a** was determined to be 10.5, which was higher than that of **1a** (1.50). This result indicates that the fluorescence on/off switching property of **2a** was more efficient than that of **1a**. It is mainly ascribed to an overlap between the absorption spectrum of diarylethene closed-ring form and the fluorescence spectrum because the fluorescence on/off switching in this work is based on RET from the fluorophore moiety to the diarylethene closed-ring form. The overlap integral (J) can be described as follows [16]:

$$J = \int f_{\mathrm{D}}(\lambda)\, \varepsilon_{\mathrm{A}}(\lambda)\, \lambda^4 \,\mathrm{d}\lambda \qquad (2)$$

where λ is the wavelength of the light, $\varepsilon_{\mathrm{A}}(\lambda)$ is the molar extinction coefficient of the acceptor, and $f_{\mathrm{D}}(\lambda)$ is the normalized fluorescence spectrum of the donor. As shown in **Fig. 4**, the overlap of the absorption spectrum of **2b** largely overlapped with the fluorescence spectrum of **2a** in comparison with that of **1a**. The J values of **2a** was estimated to be 1.58×10^{-13} $\mathrm{M^{-1}\ cm^3}$, which is larger than that of **1a** (0.61×10^{-13} $\mathrm{M^{-1}\ cm^3}$). Moreover, the Förster distance (R_0) and RET efficiency (E) were calculated as follows. The R_0 values of **1a** and **2a** in *n*-hexane were determined to be 2.29 and 2.51 nm, respectively, based on the Förster equation as follows [16]:

$$R_0{}^6 = \frac{9Q_0(ln10)\kappa^2 J}{128\pi^5 n^4 N_A} \qquad (3)$$

where Q_0 is the fluorescence quantum yield of donor in the absence of the acceptor, κ^2 is orientation factor, N_A is Avogadro constant, and n is refractive index of the medium. The E values of **1a** and **2a** in *n*-hexane were calculated to be 69 and 90%, respectively, when the distance between the diarylethene and fluorophore moieties (r_{DA}) was assumed to be 2.0 nm as follows[16]:

$$E = \frac{{R_0}^6}{{R_0}^6 + {r_{DA}}^6} \tag{4}$$

The calculated E values of **2a** is larger than that of **1a** although the Φ_f of **2a** is smaller than that of **1a**. Thus, more efficient fluorescence on/off switching of **2a** compared with that of **1a** is ascribed to larger spectral overlap.

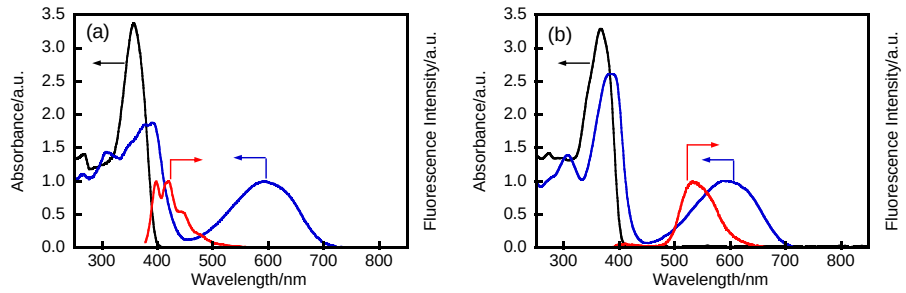

Fig. 4. Normalized absorption spectra of the open-ring form (black line) and the photostationary solution upon irradiated with 313 nm light (blue line) of **1a** (a) and **2a** (b) in *n*-hexane and normalized fluorescence spectrum upon excitation at 366 nm (red line).

Solvent effect

Next, solvent effect of the fluorescence on/off switching property for **1a** and **2a** was investigated. Even if the polarity of the solvent increased, the λ_{abs} and λ_{flu} of **1a** hardly changed as shown in **Figs. 5** and **6**. In contrast, the solvent dependence of the fluorescence spectra of **2a** was observed though the absorption spectra hardly changed by the solvents (**Figs. 7** and **8**). In toluene, a fluorescence peak was observed around 530 nm, which is ascribed to ESIPT fluorescence from the keto form, as shown in **Fig. 2a**. However, in *N*,*N*-dimethylsulfoxide (DMSO), a fluorescence peak was observed around 410 nm, which is ascribed to the presence of the enol form [31]. As shown in **Fig. 2b**, the fluorescence of the enol form is observed in polar solvents, as mentioned later in detail, because of the interaction between the hydroxy group of the enol form and the polar solvents.

Fig. 9 shows the photograph of fluorescence in various solvents upon excitation with 365 nm light. In non-polar solvent such as *n*-hexane and toluene, the green fluorescence of the keto form (ESIPT fluorescence) was observed around 530 nm, and the fluorescence of the enol form (normal fluorescence) was slightly observed around 410 nm. In contrast, in polar solvents such as methanol and DMSO, the

normal fluorescence was mainly observed. These results indicate that the ratio of keto and enol forms at excited state in the solution depended on the solvent. Two different fluorescence peaks, i.e. ESIPT and normal fluorescence, are often observed in ESIPT molecules depending on the nature of surrounding medium such as the solvent [17,32–34]. ESIPT fluorescence was predominantly observed with large Stokes shift and structureless band in hydrocarbon and non-polar solvents. On the other hand, normal fluorescence was typically observed in protic or polar solvents, which is attributed to the enol form. One of the factors that can hamper the ESIPT process is the formation of intermolecular hydrogen bonding with solvent molecules [34–37]. The formation of the intramolecular hydrogen bond is essential for the efficient ESIPT reaction since ESIPT process takes place along the reaction coordinate located on the locus of intramolecular hydrogen bond [35–38]. However, in polar or protic solvents such as DMSO, methanol, and water, both the proton donor and acceptor groups of ESIPT molecules can make intermolecular hydrogen bond with solvent molecules. Thus, the formation intramolecular hydrogen bond between the proton donor and acceptor groups of ESIPT molecules is suppressed, which results in normal fluorescence from enol form in polar or protic solvents.

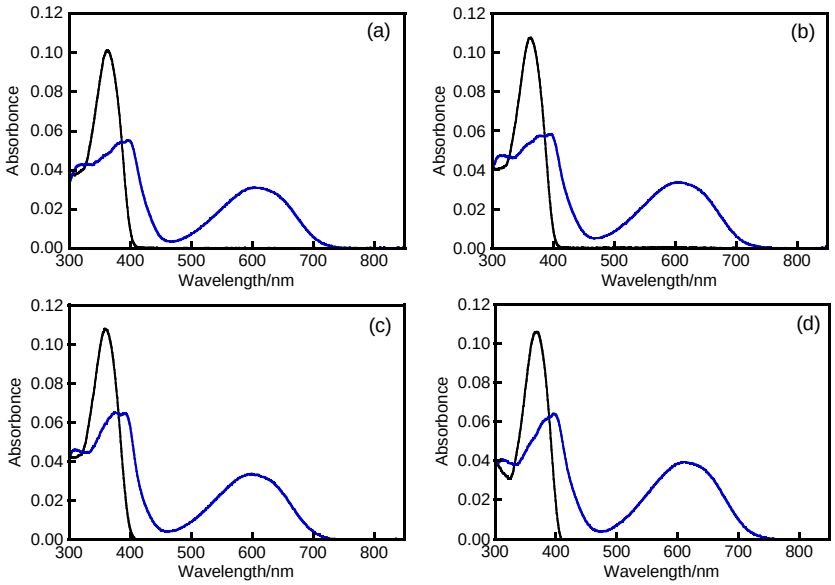

Fig. 5. Absorption spectral changes of **1a** (black solid line) and the photostationary solution upon irradiation with 313 nm light (blue dashed line) in (a) toluene, (b) THF, (c) methanol, and (d) DMSO.

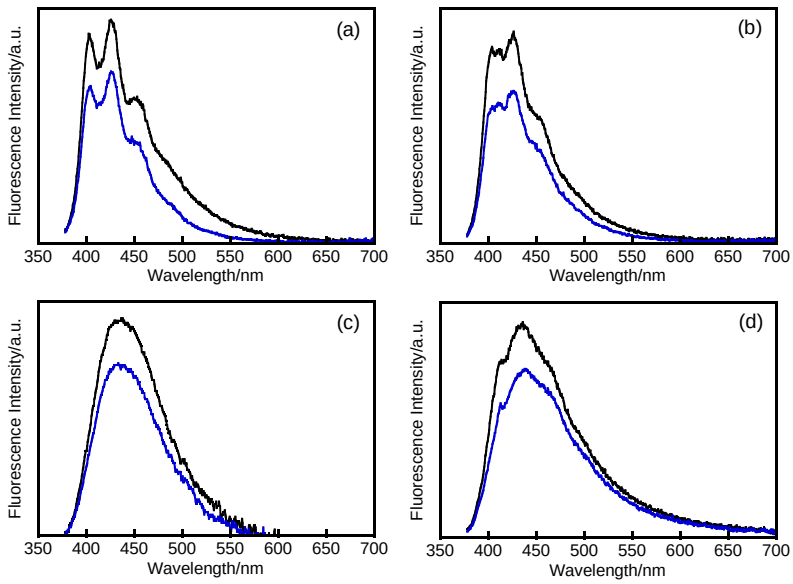

Fig. 6. Fluorescence spectral changes of **1a** (black line) and the photostationary solution upon irradiation with 313 nm light (blue line) in (a) toluene, (b) THF, (c) methanol, and (d) DMSO. The fluorescence spectra were recorded upon excitation at 366 nm.

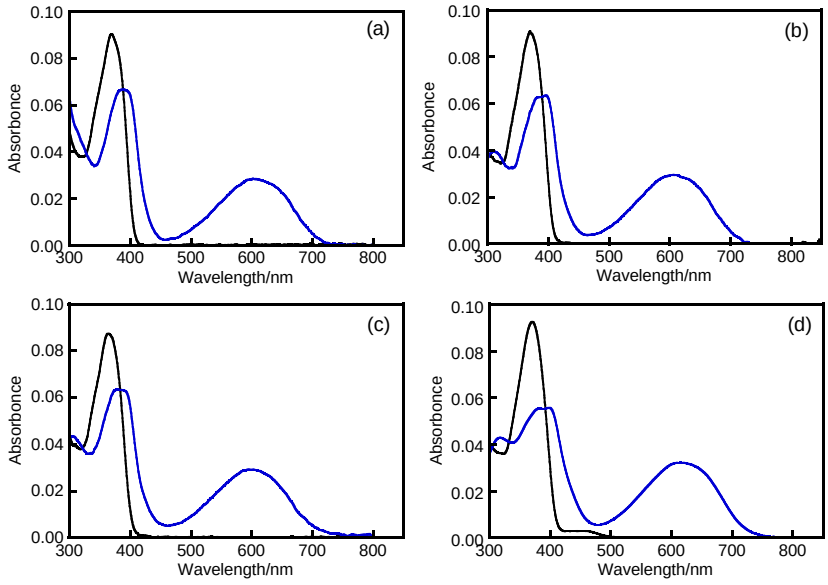

Fig. 7. Absorption spectral changes of **2a** (black line) and the photostationary solution upon irradiation with 313 nm light (blue line) in (a) toluene, (b) THF, (c) methanol, and (d) DMSO.

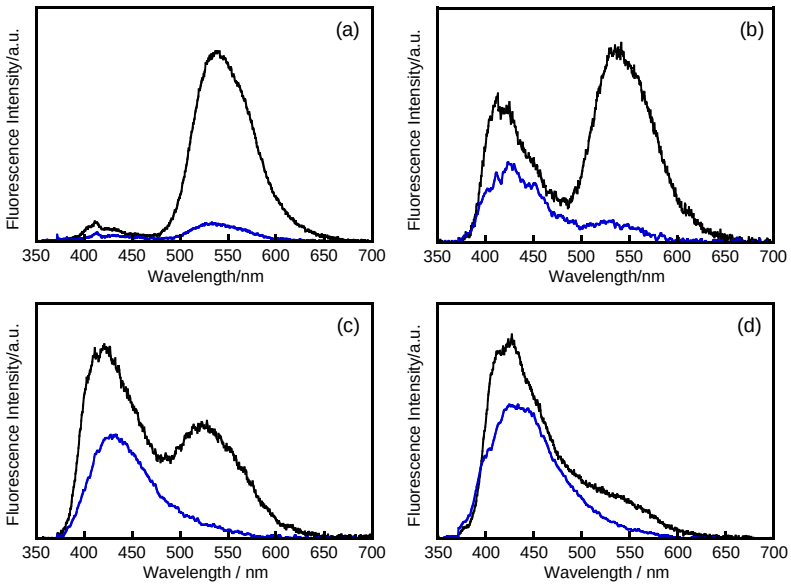

Fig. 8. Fluorescence spectral changes of **2a** (black line) and the photostationary solution upon irradiation with 313 nm light (blue line) in (a) toluene, (b) THF, (c) methanol, and (d) DMSO. The fluorescence spectra were recorded upon excitation at 366 nm.

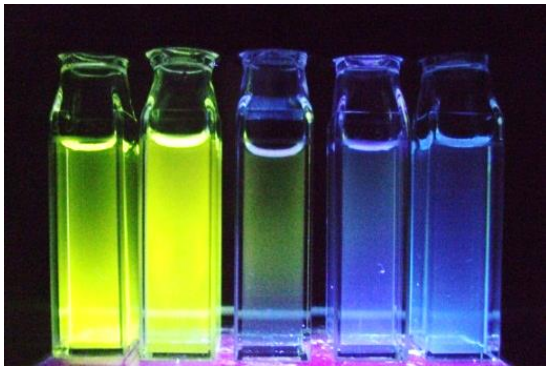

Fig. 9. Photographs of fluorescence of **2a** upon irradiation with 365 nm light as an excitation light. The solvent is *n*-hexane, toluene, THF, methanol, and DMSO from the left.

The fluorescence intensity of **1a** and **2a** gradually decreased with increasing photocyclization conversion in other solvents as well as in *n*-hexane. The fluorescence on/off contrasts of **1a** and **2a** in various solvents are summarized in **Table 2**. The fluorescence on/off contrast of **1a** hardly changed in all solvents. As mentioned above, because the fluorescence spectra of **2a** changed by the solvents, thus the spectral overlap changed, the fluorescence on/off switching property largely depended on the solvent. As shown in Fig 3, in polar solvents, RET form the enol form to the diarylethene closed-ring form is dominant

in polar solvents although the fluorescence is quenched by RET from the keto form to the diarylethene closed-ring form in non-polar solvents. The ESIPT fluorescence was almost quenched at PSS. However, the decrease in the normal fluorescence from the open-ring form to PSS was smaller than that in the ESIPT fluorescence. To quantitatively evaluate the difference of the fluorescence on/off contrast between the ESIPT and normal fluorescence regions, the fluorescence spectra was divided into two regions as shown in **Fig. 10**; 480 nm was defined as the boundary line. The fluorescence spectra of longer and shorter wavelength regions than 480 nm were defined as the ESIPT and normal fluorescence, respectively. In all solvents, the fluorescence on/off contrasts in ESIPT fluorescence region were higher than those in normal fluorescence region. These results are ascribed to the overlap between the absorption spectra in the closed-ring form and the fluorescence spectra. The normal fluorescence hardly overlapped with the absorption spectra of **2b** in comparison with the ESIPT fluorescence, which results in the low fluorescence on/off contrast in normal fluorescence region. Moreover, the fluorescence on/off contrast values for the total fluorescence in non-polar solvents were higher than those in polar solvents because the relative fluorescence intensity of the ESIPT fluorescence increased in non-polar solvent. As a result, the fluorescence on/off switching property in non-polar solvents were more efficient than those in polar solvents.

Table 2. Fluorescence on/off contrast and fluorescence quantum yield of **1a** and **2a** in various solvents.

Solvent	Φ_f (λ_{flu}/nm)		Fluorescence on/off contrast			
			1a	**2a**		
	1a	**2a**		Nor. Flu.	ESIPT Flu.	Total Flu.
n-Hexane	0.015 (398, 417)	0.010 (411, 534)	1.50	3.4	12.3	10.5
Toluene	0.013 (403, 426)	0.0089 (413, 538)	1.51	2.5	10.7	8.1
THF	0.0071 (402, 426)	0.0074 (416, 536)	1.39	1.7	8.4	3.0
Methanol	0.011 (437))	0.0051 (420, 524)	1.30	1.9	5.7	2.5
DMSO	0.012 (436)	0.0058 (427, 517)	1.22	1.3	2.1	1.4

[a] Fluorescence spectra from 350 to 480 nm. [b] Fluorescence spectra from 480 to 700 nm.

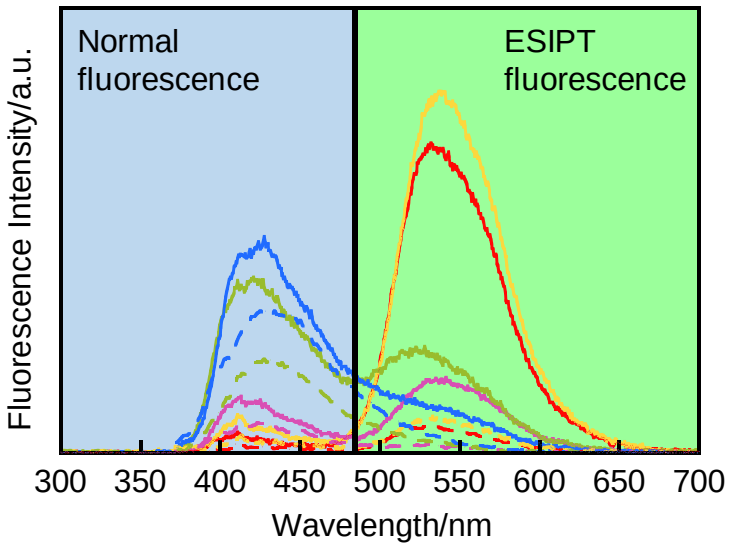

Fig. 10. Fluorescence spectral changes of **2a** in *n*-hexane (red), toluene (yellow), THF (purple), methanol (green), and DMSO (blue): open-ring form (solid line) and the photostationary solution upon irradiation with 313 nm light (dashed line). The fluorescence spectra were recorded upon excitation at 366 nm.

Conclusion

We synthesized fluorescence photoswitchable diarylethenes **1a** and **2a**. Diarylethenes **1a** and **2a** exhibited reversible photochromic reactions and fluorescence on/off switching upon alternating irradiation with UV and visible light. Diarylethene **2a** has more efficient fluorescence on/off switching property in comparison with **1a** because the fluorescence on/off contrast of **2a** was higher than that of **1a**. This is due to the large spectral overlap between the absorption spectrum of **2b** and fluorescence spectrum of **2a**. Moreover, the fluorescence on/off switching property of **2a** depended on the polarity of the solvents. In non-polar solvents such as *n*-hexane and toluene, ESIPT fluorescence of keto form was mainly observed though normal fluorescence of enol form was significantly observed in polar solvents such as DMSO and methanol. The fluorescence on/off contrasts in polar solvents were much lower than those in non-polar solvents, which is also ascribed to the spectral overlap between the absorption spectrum of **2b** and fluorescence spectrum of **2a**. Thus, the fluorescence on/off switching property of **2a** was greatly affected to the polarity of the solvents.

Acknowledgments This work was partly supported by JSPS KAKENHI Grant Number JP26107013 in Scientific Research on Innovative Areas “Photosynergetics” and JSPS KAKENHI Grant Number JP16K17896 in Scientific Research for Young Scientists (B). The authors also thank Osaka Gas Chemical Co., Ltd. and Nippon Zeon Co., Ltd. for providing chemicals.

References

1. S.-Z. Pu, Q. Sun, C.-B. Fan, R.-J. Wang, G. Li, J. Mater. Chem. C **4**, 3075 (2016).
2. Z. Yang, J. Cao, Y. He, J. H. Yang, T. Kim, X. Peng, J. S. Kim, Chem. Soc. Rev. **43**, 4563 (2014).
3. E. Betzig, G. H. Patterson, R. Sougrat, O. W. Lindwasser, S. Olenych, J. S. Bonifacino, M. W. Davidson, J. Lippincott-Schwartz, H. F. Hess, Science **313**, 1642 (2006).
4. S. T. Hess, T. P. K. Girirajan, M. D. Mason, J. Biophys. **91**, 4258 (2006).
5. P. Sengupta, S. B. van Engelenburg, J. Lippincott-Schwartz, Chem. Rev. **114**, 3189 (2014).
6. T. Fukaminato, S. Kobatake, T. Kawai, M. Irie, Proc. Jpn. Acad., Ser. B **77**, 30 (2001).
7. C. C. Corredor, Z. -L. Huang, K. D. Belfield, Adv. Mater. **18**, 2910 (2006).
8. C. C. Corredor, Z.-L. Huang, K. D. Belfield, A. R. Morales, M. V. Bondar, Chem. Mater. **19**, 5165 (2007).
9. C. Yun, J. You, J. Kim, J. Huh, E. Kim, J. Photochem. Photobiol. C **10**, 111 (2009).

10. T. Fukaminato, T. Doi, N. Tamaoki, K. Okuno, Y. Ishibashi, H. Miyasaka, M. Irie, J. Am. Chem. Soc. **133**, 4984 (2011).
11. M. Irie, T. Fukaminato, T. Sasaki, N. Tamai, T. Kawai, Nature **420**, 759 (2002).
12. T. Fukaminato, J. Photochem. Photobiol. C **12**, 177 (2011).
13. M. Irie, T. Fukaminato, K. Matsuda, S. Kobatake, Chem. Rev. **114**, 12174 (2014).
14. L. Giordano, T. M. Jovin, M. Irie, E. A. Jares-Erijman, J. Am. Chem. Soc. **124**, 7481 (2002).
15. R. Métivier, S. Badré, R. Méallet-Renault, P. Yu, R. B. Pansu, K. Nakatani, J. Phys. Chem. C **113**, 11916 (2009).
16. I. Medintz, N. Hildebrandt, FRET–Förster resonance energy transfer from theory to applications; Wiley-Interscience: New York, 2013; pp 25−31.
17. J. E. Kwon, S. Y. Park, Adv. Mater. **23**, 3615 (2011).
18. S.-J. Lim, J. Seo, S. Y. Park, J. Am. Chem. Soc. **128**, 14542 (2006).
19. D. Kim, J. E. Kwon, S. Y. Park, Adv. Optical Mater. **4**, 790 (2016).
20. C. Li, H. Yan, L.-X. Zhao, G.-F. Zhang, Z. Hu, Z.-L. Huang, M.-Q. Zhu, Nature Commun. **5**, 5709 (1–11) (2014).
21. X. Donga, R. Wanga, G. Liua, P. Liua, S. Pu, Tetrahedron **72**, 2935 (2016).
22. M. Irie, T. Lifka, S. Kobatake, N. Kato, J. Am. Chem. Soc. **122**, 4871 (2000).
23. Y. Yokoyama, Y. Kurita, J. Synth. Org. Chem. Jpn. **49**, 364 (1991).
24. C. A. Parker, W. T. Rees, Analyst **85**, 587 (1960).
25. W. R. Dawson, M. W. Windsor, J. Phys. Chem. **72**, 3251 (1968).
26. W. H. Melhuish, J. Phys. Chem. **65**, 229 (1961).
27. S. Hamai, F. Hirayama, J. Phys. Chem. **87**, 83 (1983).
28. S. R. Meech, D. Phillips, J. Photochem. **23**, 193 (1983).
29. M. N. Roberts, J. K. Nagle, J. G. Finden, N. R. Branda, M. O. Wolf, Inorg. Chem. **48**, 19 (2009).
30. M. S. Maji, T. Pfeifer, A. Studer, Chem.–Eur. J. **16**, 5872 (2010).
31. S.-G. Roh, Y.-H. Kim, K. D. Seo, D. H. Lee, H. K. Kim, Y.-I. Park, J.-W. Park, J.-H. Lee, Adv. Funct. Mater. **19**, 1663 (2009).

32. D. D. Pant, H. C. Josh, P. B. Bisht, H. B. Tripathi, Chem. Phys. **185**, 137 (1994).

33. P. B. Bisht, H. B. Tripathi, D. D. Pant, J. Photochem. Photobio. A: Chem. **90**, 103 (1995).

34. P.-T. Chou, M. L. Martinez, J. H. Clements, J. Phys. Chem. **97**, 2618 (1993).

35. M. H. Van Benthem, G. D. Gillispie, J. Phys. Chem. **88**, 2954 (1984).

36. M. Kasha, *J. Chem. Soc*., Faraday Trans. 2 **82**, 2379 (1986).

37. D. McMorrow, M. J. Kasha, J. Am. Chem. Soc. **105**, 5133 (1983).

38. A. J. G. Strandjord, P. F. Barbara, J. Phys. Chem. **89**, 2355 (1985).